

Study of flare energy release using events with numerous type III-like bursts in microwaves

Solar Physics

N.S. Meshalkina¹ · A.T. Altyntsev¹ ·
D.A. Zhdanov¹ · S.V. Lesovoi¹ ·
A.A. Kochanov¹ · Y.H. Yan² · C.M. Tan² ·

© Springer ●●●

Abstract The analysis of narrowband drifting of type III-like structures in radio bursts dynamic spectra allows to obtain unique information about primary energy release mechanisms in solar flares. The SSRT spatially resolved images and a high spectral and temporal resolution allow direct determination not only the positions of its sources but also the exciter velocities along the flare loop. Practically, such measurements are possible during some special time intervals when the SSRT (about 5.7 GHz) is observing the flare region in two high-order fringes; thus, two 1D scans are recorded simultaneously at two frequency bands. The analysis of type III-like bursts recorded during the flare 14 Apr 2002 is presented. Using-multiwavelength radio observations recorded by SSRT, SBRS, NoRP, RSTN we study an event with series of several tens of drifting microwave pulses with drift rates in the range from -7 to 13 GHz s^{-1} . The sources of the fast-drifting bursts were located near the top of the flare loop in a volume of a few Mm in size. The slow drift of the exciters along the flare loop suggests a high pitch-anisotropy of the emitting electrons.

Keywords: Solar flares; Radio bursts; Microwave emission; Dynamic spectrum; Drifting bursts

1. Introduction

During solar flares a large amount of stored magnetic field energy is suddenly released, and transformed into heat, mass motions, enhanced emission of electromagnetic radiation, and enhanced fluxes of energetic particles. Radio emission reveals the presence of nonthermal electrons, both in the acceleration region and along their propagation path. In a recent study by Fleishman *et al.* (2011)

¹Institute of Solar-Terrestrial Physics SB RAS, Lermontov St. 126A, Irkutsk 664033, Russia email: nata@iszf.irk.ru

² Key Laboratory of Solar Activity, National Astronomical Observatories, CAS, Beijing 100012, China e-mail: yyh@bao.ac.cn

these two mentioned above components were identified in the observational data and carefully separated. Major results on the propagation of electron beams have been obtained studying drifting bursts of the so-called type III, which are characterized as narrow-band bursts whose frequency either rapidly increases or drops with time. It is generally accepted that the emission exciter frequency of type III bursts is determined by the local plasma frequency, which is proportional to the square root of the plasma density. Furthermore, a drift with decreasing frequency is explained by the propagation of the electron beams from the solar surface toward decreasing plasma density, and an increase in frequency with time will correspond to a downward movement (Robinson and Benz, 1992; Aschwanden, 2002).

It is assumed that structures of subsecond duration (< 1 s) in radio emission are indicators of primary energy release processes in solar flares. One of the probable mechanisms of the generation of observable individual pulses in trains is the reconnection process (Kliem, 1989, 1995; Kliem, Karlicky, and Benz, 2000; Machado *et al.*, 1993; Aschwanden, 1993, 2004). Radio bursts with fine temporal structure and their response in HXR and radio emission have been studied for more than 20 years (Aschwanden and Gudel, 1992; Aschwanden, Dennis, and Benz *et al.*, 1998; Huang, Fu, and Qin, 1999; Benz, 2006). Although, as a rule, there is no unambiguous correlation between the microwave profiles and the HXR pulses, on the subsecond time-scale of subsecond pulses (SSP) agrees with HXR intensity increases. Although SSPs are almost always associated with HXR emission, the reverse is not true. HXR bursts are accompanied by subsecond pulses very rare. This suggests the existence of some special boundary conditions for a temporal fine structure to be generated and for the emission to escape from the generation site.

Observations of subsecond pulses characterised by narrow-band coherent emission provide a promising way to estimate the plasma parameters at acceleration sites. Using one-dimensional brightness distribution recorded with the *Siberian Solar Radio Telescope* (SSRT) interferometer in adjacent high-order fringes we can measure the exciter displacement at two different frequencies near 5.7 GHz in direction perpendicular the interference fringe pattern. Thus, it is possible to measure the exciter velocity and plasma density gradient along one direction in the image plane.

Characteristics of drifting bursts in microwave range considerably differ from the well-studied metric bursts of type III. At high plasma densities a key question whether emission is detectable despite the strong free-free absorption in the dense plasma surrounding the fast-drifting exciter. Emission at the plasma frequency cannot escape from the source. Weaker absorption at the doubled plasma frequency can be estimated (Dulk, 1985; Benz, 1993) as $\exp^{-\tau}$, where:

$$\tau = 0.12 \left(\frac{f}{1\text{MHz}} \right)^2 \left(\frac{T}{1\text{MK}} \right)^{-3/2} \left(\frac{H}{1\text{Mm}} \right) \quad (1)$$

where H is the transverse scale of variation in density, T is plasma temperature in the emission source, f is frequency of the observed radio emission.

The SSRT observations with spatial resolution confirm that the observed emission frequency of the fast-drifting bursts is close to the doubled plasma frequency determined by the sources' plasma density (Meshalkina *et al.*, 2004). For emission at the SSRT working frequency (5.7 GHz) the exciter plasma density should exceed 10^{11}cm^{-3} and density scale height H should be less than thousand km. This width is lower than the flare loop's cross-sections observed in UV and X-rays. A favorable condition to observe the coherent microwave emission is realized when the source is located at large height near the top of the dense hot loop so that the electromagnetic waves can escape across the flare loop. Really, in the majority of events with the subsecond pulses the sources have been located near loop tops (Meshalkina *et al.*, 2004).

At high frequencies the positive drifts are predominant. This direction of a frequency drift can be naturally explained by the exciter moving from a loop top to denser plasma in the legs of the loop. Observations of a specific type of the fast-drifting bursts, so called U-bursts, shows, that the apparent frequency drifts can be caused not only by an exciter moving through a density gradient, but by a change of density in a steady emission source (Altyntsev *et al.*, 2003a). So, to interpret fast-drifting bursts in the microwaves we should distinguish between effects of temporal and spatial changes of plasma density. In this context the analysis of the events with a large number of fast-drifting bursts is promising.

Note that spatially-resolved trains of short drifting bursts are very rarely recorded simultaneously with their dynamic spectra: until now, the only such event was found on 30 March 2001 (Altyntsev *et al.*, 2007). For a half-minute interval, the drift rates of 67 drifting subsecond pulses were -10 to 20 GHz s^{-1} and widely scattered around an average value of 6 GHz s^{-1} . The estimated exciter velocities from the drift rates, without correcting for this mean, results were in a wide range, some even exceeding the speed of light. To solve this discrepancy, it was suggested that the overall drift was due to increase of density at the emission site. Plasma influx can result from a magnetic reconnection process. For the one-dimensional approximation (Sweet-Parker model) the current-sheet thickness should be of order 20 m and the reconnection rate $\alpha \approx 3.6 \times 10^{-5}$ of the Alfvén velocity.

Recently, we discovered a second event (14 Apr 2002) with a large number of drifting bursts recorded simultaneously with the SSRT interferometer (at two frequencies) and the Chinese spectropolarimeter. The presence of a large number of drifting bursts gives us the chance to extract the component of frequency drift reflecting a plasma density increase in the emission region. The purpose of this study is to analyze the 14 Apr 2002 event and compare the results for the two events as well as estimating the plasma parameters in the fast drifting burst sources.

2. Instruments

The dynamic spectra of the microwave burst were recorded with the *Solar Broadband Radio Spectrometer* (SBRS, 5.2 – 7.6 GHz) at the Huairou Solar Observing Station of the National Astronomical Observatories of China (Fu *et al.*, 1995). ■

The single-channel bandwidth of the SBRs is 20 MHz, and the temporal resolution is 5 ms (Ji *et al.*, 2003). We used the SBRs total flux records to extract individual bursts.

The spatial structures were recorded with the SSRT (Grechnev *et al.*, 2003). The SSRT consists of two linear antenna arrays – East - West (EW) and North - South (NS) – and operates in the 5.67 – 5.79 GHz range. The right – (RCP) and left-handed (LCP) circularly polarized components are recorded alternately, 7 ms each. The SSRT produces two-dimensional full-disk images every 3 – 5 min, and observes microwave bursts in the one-dimensional (1D) mode with the EW and NS linear interferometers independently. The 1D mode has a temporal resolution of 14 ms. The time profiles of radio flux variation in the intensity ($I=R+L$) and circular polarization ($V=R-L$) channels are posted on a regular basis, at the Institute of Solar-Terrestrial Physics Radio Astronomical Observatory website¹.

The SSRT receiver system is a 120-MHz-band spectrum analyzer implemented as an acousto-optic receiver. It has 250 frequency channels, which correspond to fans of knife edge beams for the NS and EW arrays. The bandwidth of a single frequency channel is 0.48 MHz. The response at each frequency corresponds to emission from a narrow strip on the solar disk, whose position and width depend on the frequency. During the event under study, the NS beam was 24.3 arc sec, the EW beam 15.3 arc sec wide.

The microwave data were taken from the *Nobeyama Radio Polarimeters* (NoRP, Torii *et al.*, 1979; Shibasaki *et al.*, 1979; Nakajima *et al.*, 1985). The NoRP measures the fluxes at 1, 2, 3.75, 9.4, 17, 35, 80 GHz with a temporal resolution of 1 s for steady mode and 0.1 s for flare mode. The Nobeyama Radioheliograph (NORH, Nakajima *et al.*, 1994) observed the flare at 17 and 34 GHz. The cadence of the data used here is 0.1 s. The NoRH beam sizes were $11 \times 17''$ at 17 GHz and $8 \times 11''$ at 34 GHz at the time of the flare.

We also used the *Radio Solar Telescope Network* (RSTN) data. One-second temporal resolution data were taken at eight frequencies (0.245, 0.41, 0.61, 0.14, 0.27, 0.5, 0.88, 15.4 GHz) from Learmonth station, Australia. We used GOES data and extreme ultraviolet (EUV) observations of the lower corona by the EIT (195 Å) (Delaboudinire *et al.*, 1995) onboard the SOHO. SOHO/MDI (Scherrer *et al.*, 1995) magnetograms represent photospheric magnetic fields.

3. Data analysis

The SSRT can simultaneously register a flare region in two interference orders at different frequencies of the SSRT band turning on the observing direction to the baselines (Grechnev *et al.*, 2003). The NS interferometer observed the 14 April 2002 flare region in two high-order fringes; thus, two 1D scans were recorded simultaneously within two frequency intervals centered at about 5.67 and 5.76 GHz. The EW linear interferometer recorded the 1D data at 5.69 GHz. The methods to analyze 1D SSRT scans have been described by

¹<http://www.ssrt.org.ru/> and <http://ssrt.iszf.irk.ru/fast/>

Altyntsev, Grechnev, and Konovalov (1996) and Altyntsev et al. (2003a, 2007). The apparent sizes of pulse sources are exceeded the real sizes and are determined by the SSRT beam size and by wave scattering in the low corona (Altyntsev, Grechnev, and Konovalov, 1996; Meshalkina *et al.*, 2005). The accuracy in measuring a relative displacement of a source recorded simultaneously at two different frequencies is estimated to be within 2 arcsec. This accuracy is achieved by measuring their centroids, and it was verified by modeling of the response with the observed noise level.

We have extracted 56 pulses from the dynamic spectrum of SBRS crossing the SSRT band (5.67 – 5.79 GHz) during a time interval of 30 sec (05:36:26 – 05:36:56). For each pulse we estimated displacements relative to the background burst.

4. Observations

The 14 April 2002 impulsive flare occurred during the interval 05:36 – 05:48 UT, with an SXR maximum of C5.3 at 05:37 UT. The flaring active region AR9907 was located at S03E45.

Subsecond microwave structures occurred at 5.2 – 7.6 GHz during the one-minute interval of the flare rise phase. According to GOES data the narrow-band structures have appeared after an abrupt increase of temperature 4 up to 10 MK and the emission measure rise to $8 \times 10^{47} \text{cm}^{-3}$ (Figure 1a). The HXR data (RHESSI) were not available for this period.

From the SBRS dynamic spectrum we have extracted 56 bursts, whose flux exceed 3σ and were recorded within the SSRT band (Figure 1). Comparison between RCP and LCP signals shows that the background burst was weakly polarized at 5.7 GHz (under to 5%), whereas subsecond pulses were pronouncedly left-polarized. Noteworthy is the high degree of agreement between the time profiles from SBRS and SSRT. The drifting structures occurred in the entire SBRS frequency range and the total spectral width of the individual bursts was found to be up to 1.5 GHz.

Figure 2a shows an example of a fast-drifting burst dynamic spectrum and the SSRT time profiles at two frequencies from 05:36:39.7 to 05:36:40.1. The horizontal dashed lines mark the frequencies of 5.67 and 5.76 GHz, at which the NS linear interferometer observed the burst. Figure 2b shows LCP emission component at two SSRT frequencies. The positions of the impulsive source centroids are shown in Figure 2c at moments when the sources are observed at the SSRT frequencies. The positions are calculated automatically for the intervals when the rapidly drifting flux component exceeds 10% of the gradual background burst. In this example the fluxes were sufficiently large in the interval marked by the vertical lines and the centroid of its 1D image at 5.67 GHz was displaced by about $3''$ relative to the background burst centroid.

The simultaneous records at two SSRT frequencies gave us a rare opportunity to estimate the plasma density gradient and velocity of exciter independently. For each pulse we defined the SSP position using the localization technique for sources of temporal fine structure (Meshalkina *et al.*, 2004) as well as their displacements and drift rates.

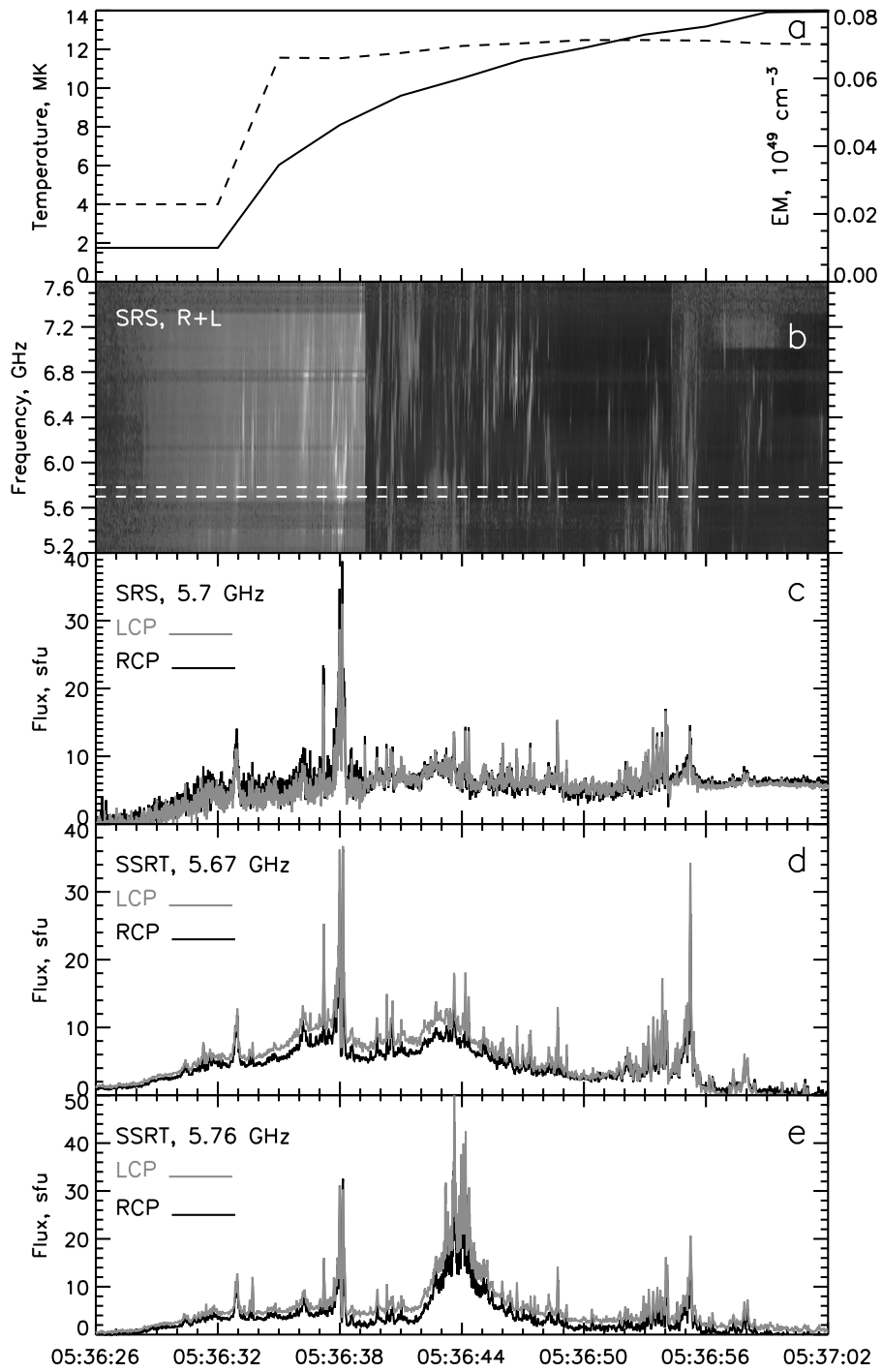


Figure 1. a) temperature (dashed line) and emission measure (solid line)(GOES10 data); b) dynamic spectrum in intensity (5.2 - 7.6 GHz, SBRs); c) RCP and LCP time profiles from the spectropolarimeter at the central frequency of SSRT band; (d), (e) RCP and LCP time profiles at two frequencies recorded with SSRT.

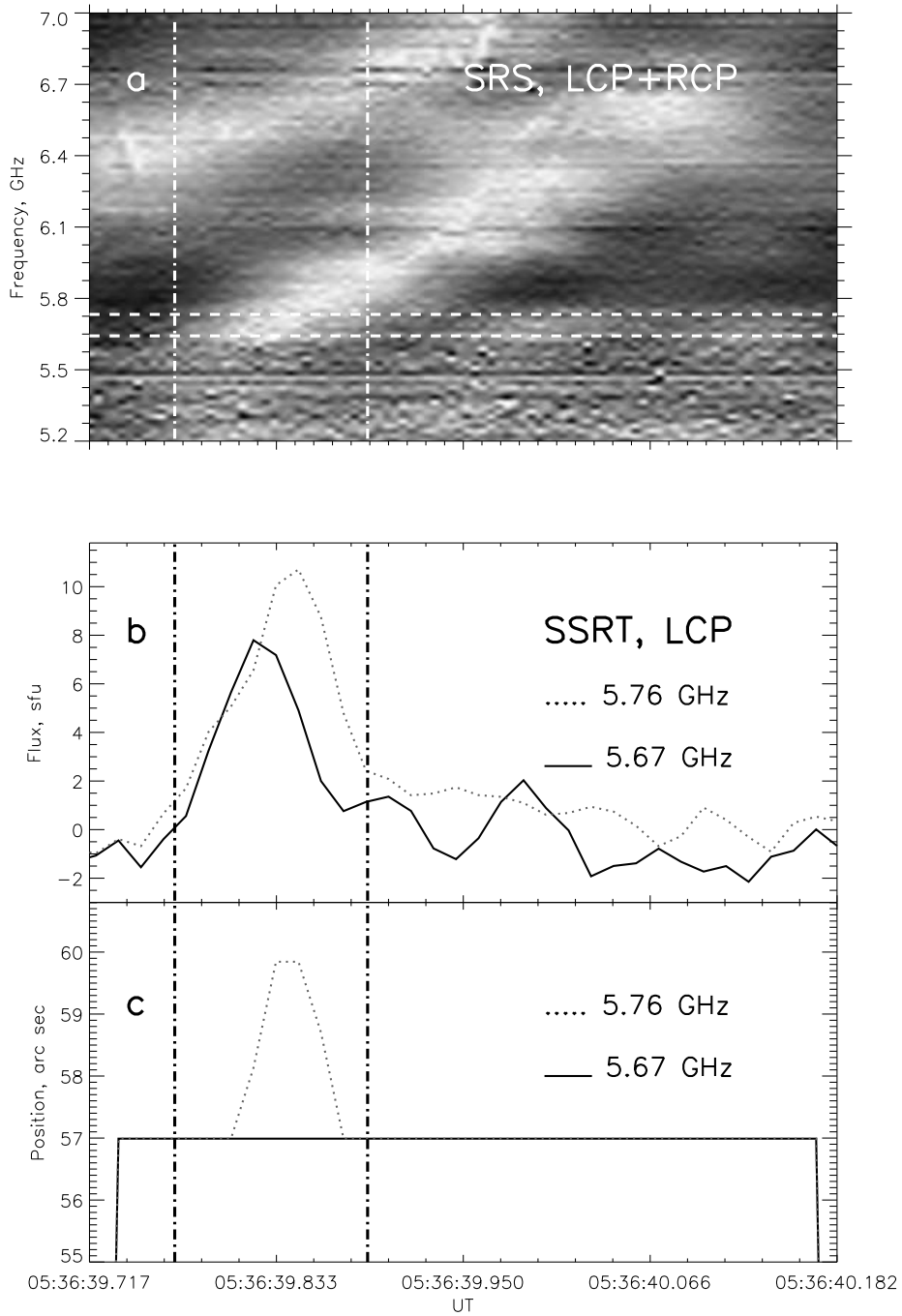


Figure 2. Observations on 14 April 2002. A subsecond pulse recorded at two frequencies. (a) Dynamic spectrum, 5.2 - 7.0 GHz band (Stokes I, SBRs). Horizontal dashed lines show the SSRT observing band. (b) Time profiles at 5.76 GHz (dotted) and 5.67 GHz (solid). (c) Positions of subsecond sources (centroids) observed at the two SSRT frequencies vs. time. Vertical dash-dotted lines indicate the SSP interval.

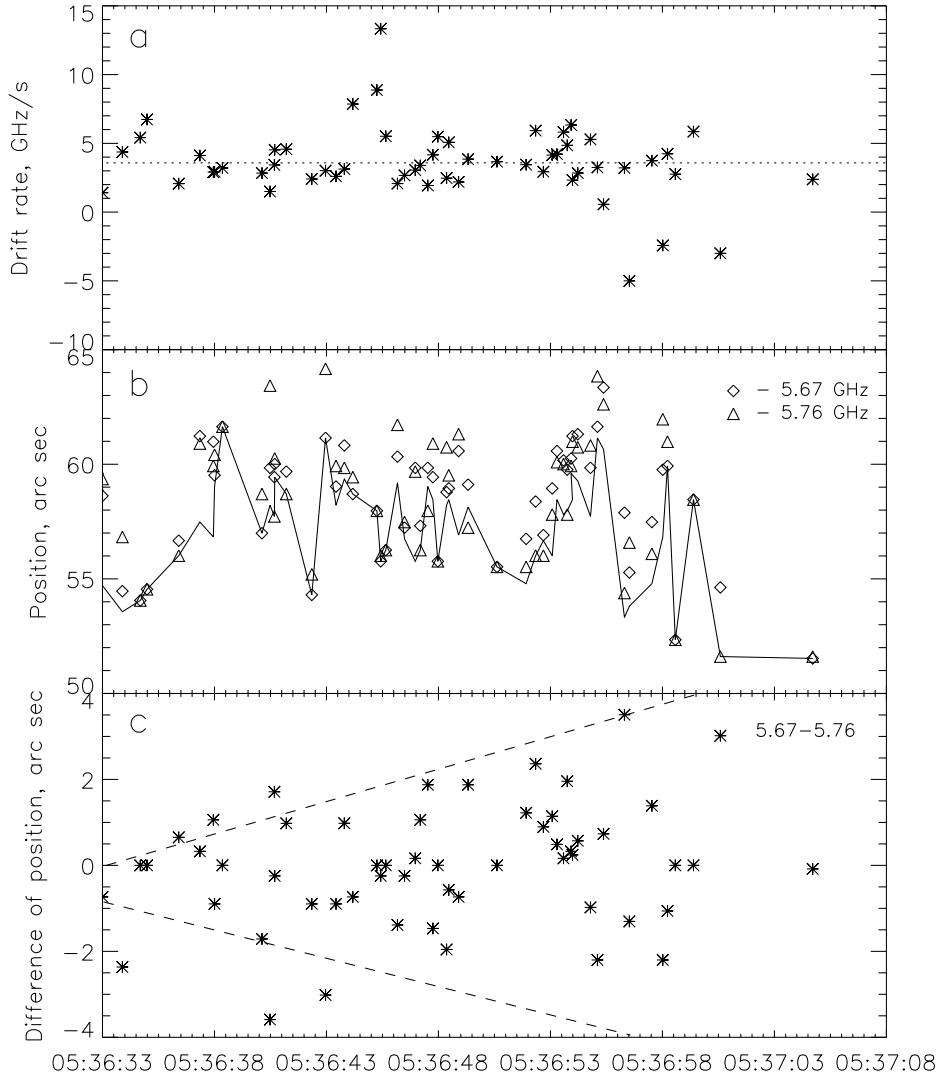


Figure 3. a) Drift rates (horizontal dotted line marks the mean value); b) Displacements of impulsive sources in 1D scans at 5.67 GHz (diamonds) and at 5.76 GHz (triangles). The solid line shows centroids of the background burst; c) Absolute values of difference between positions at two frequencies.

Measurements for the pulses are shown in Figure 3. The scatter of drift rates is obviously random in time and distributed around the average value 3.6 GHz s^{-1} (Figure 3a) except the four pulses. During the 2001 April 14 event drifting bursts were observed at the frequencies of 5.67 and 5.76 GHz ($\Delta f = 0.09 \text{ GHz}$). The 1D brightness distributions were recorded every 14 ms in a direction perpendicular to the NS line in Figure 4 and show the spatial characteristics along

the flare loop. The position variation of the background burst provides guidance on accuracy of absolute spatial measurements (Figure 3b). The positions of the drifting burst sources were measured relative to the co-temporal burst centroid. The spaces between the "gravity" centers of pulse sources in 1D data recorded at different frequencies show the projected displacement (Δl) of the exciter. It is seen that spatial scatter of displacement Δl is increasing in time (dashed lines at Figure 3c). So, the density profile was likely to flatten out along the loop.

The spatial structure of the flare is shown in Figure 4. The microwave image at 5.7 GHz shows a loop, lying approximately along the northwest direction. The negatively polarized source (LCP) at 17 GHz was located near the northern footpoint of the loop as observed in UV (Figure 4a). The apparent sizes of subsecond pulse sources were below the SSRT beam width, microwave burst size was about $25''$.

The centroids of both the background and impulsive emissions were located close to the loop top. Centroids of the fast drifting sources were located within the blue dotted frame of $5 \times 7''$. The distance between the loop footpoints was about $45''$ as seen in UV.

The spectrum of the microwave burst was calculated using the code of Fleishman and Kuznetsov (2010) and parameters from observational data (area is $1.3 \times 10^{19} \text{ cm}^2$, thickness is $3.6 \times 10^9 \text{ cm}$) (Figure 5). A satisfactory fitting can be obtained based on the following reasonable parameters: plasma temperature 10 MK and density $1.1 \times 10^{10} \text{ cm}^{-3}$, electron spectrum exponent 4, density of nonthermal electrons with over 16 keV energies $8 \times 10^6 \text{ cm}^{-3}$, magnetic field 70 G, line of sight 80 degrees to the magnetic field direction.

5. Discussion

The fast drifting bursts were observed in the total SBRS range from 5.2 up to 7.5 GHz. It is well established that the frequencies of fast drifting burst in microwaves are close to the local harmonic Langmuir frequency (Fleishman and Melnikov, 1998; Altyntsev *et al.*, 2000; Benz, 2000). So the plasma density was in the range of $(1 - 2) \times 10^{11} \text{ cm}^{-3}$ in the emission volume during the total time interval with the fine spectral structures.

The emission region was located near the loop top within the $5 \times 7''$ frame. The projected displacement along the loop (Figure 3) were small in most events and as a rule did not exceed the measurement accuracy of two arcseconds. So, the longitudinal size of emission region was small in comparison with the loop length and did not exceed three-five thousand km. This contradicts the usual interpretation of positive drifting bursts by exciter moving from loop top towards denser loop foot points.

Using the emission measure EM calculated from GOES data and assuming a cylindrical shape of emission region we can estimate the radius value as $(1 - 2) \times 10^8 \text{ cm}$ for the emission value of $5 \times 10^{47} \text{ cm}^{-3}$. Here we have taken the cylinder length of $3 \times 10^8 \text{ cm}$ and plasma density of $(1 - 2) \times 10^{11} \text{ cm}^{-3}$. It is an over-estimation because we assume that the increase of the GOES signals was due to the dense emission region. The calculated sizes agree with the frame bounded

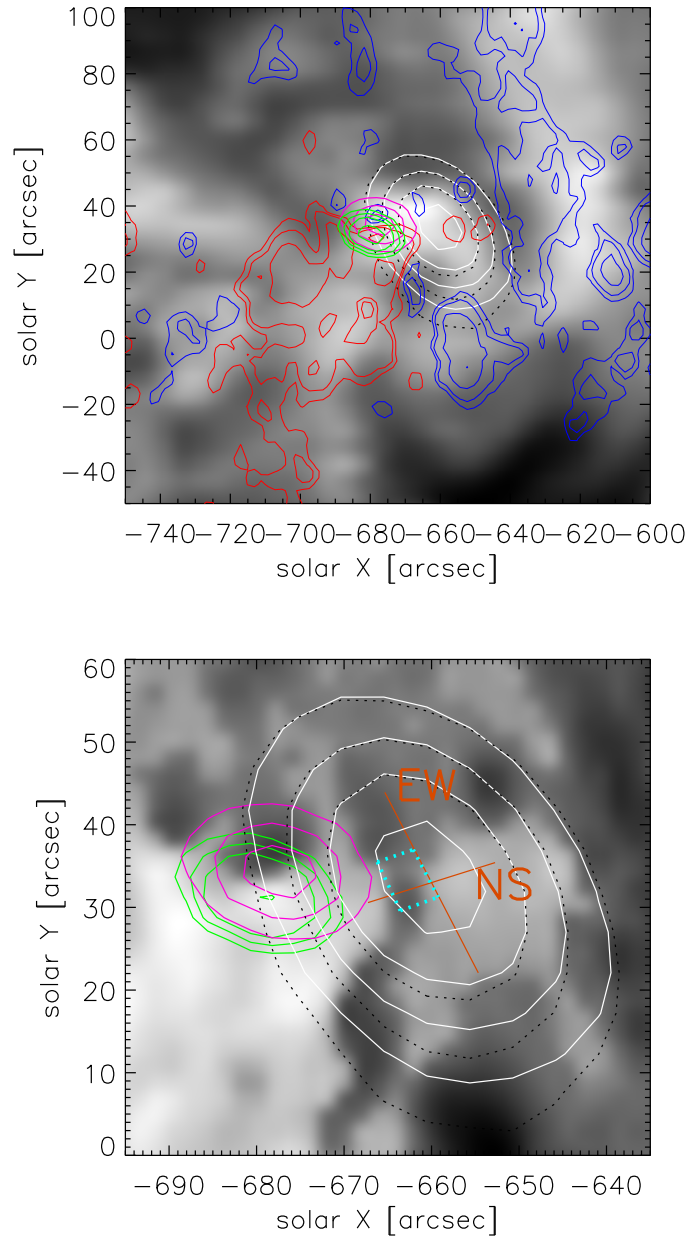


Figure 4. Top: Contours of 5.7 GHz (SSRT, difference between images at 05:36 and 05:34) are sources (white solid: Stokes I, 30%, 50%, 70%, 90% of the maximum; black dotted: Stokes V, LCP, 30%, 50%, 70% of the maximum). Pink contours: Stokes I, (NoRH, 17 GHz, 05:37, 50%, 70%, 90% of the maximum); green contours: Stokes V(NoRH, 17 GHz, 05:37, 50%, 60%, 70%, 90% of the minimum) superimposed on an EIT image 195 Å (05:36:05). The axes show arc sec from the solar disk centre. Red contours represent positive polarity of MDI magnetogram (06:24:30), blue contours show negative polarity (levels $\pm 100G$, $\pm 200G$, $\pm 500G$, $\pm 1000G$, $\pm 1500G$). Bottom: Enlarged part of image in panel (a). The meaning of contours and levels are the same. Background is MDI magnetogram (06:24:30, light areas denote positive polarity; dark areas negative polarity). The blue frame restricts the scatter of positions of subsecond pulse sources. The orange lines show the scan directions of the SSRT linear interferometers.

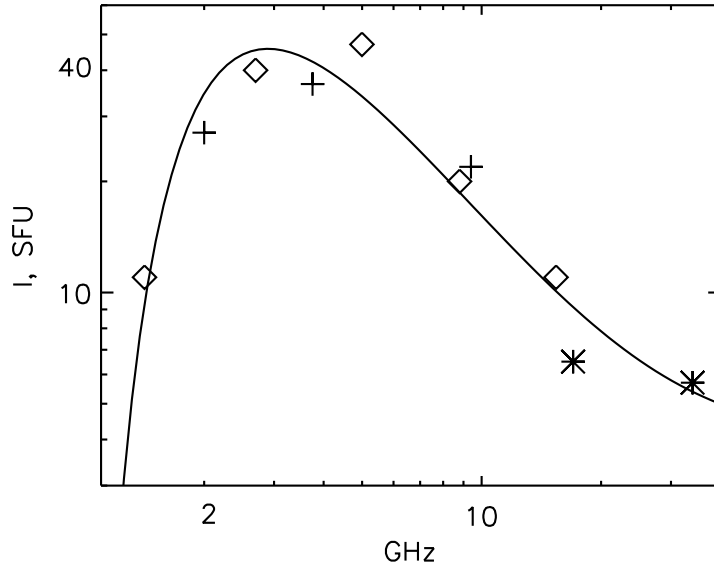


Figure 5. Spectrum of the background microwave burst during observations of type III bursts (05:36:41.00). Crosses are for data from NoRP spectropolarimeters; diamonds denote the Learmonth observatory of the RSTN network; asterisks stand for fluxes obtained by integrating brightness temperatures over sequences of NoRH flare region images at 17 and 34 GHz. The solid curve shows calculation results for gyrosynchrotron and bremsstrahlung using the code by Fleishman and Kuznetsov (2010).

in Figure 4c. Note that the position scattering of the fast-drifting sources was gradually rising along the loop (Figure 3c). So, the density profile along the loop is flattening out at the approximately constant level and the GOES emission measure growth was caused by the dense region expansion.

The recorded fast-drifting bursts have started after the temperature rising up to 10 MK. Using the Equation (1) and taking $H = 3 \times 10^8$ cm we estimated that this region became optically thin ($\tau < 1$) at this time. The dense emitting region was surrounded by a low-density plasma as follows from the fitting of the continuum burst spectrum.

The frequency drift rate, df/dt , is determined by the expression:

$$df/dt = \frac{A}{2\sqrt{n}} \frac{dn}{dt} = \frac{A}{2\sqrt{n}} \left(\frac{\partial n}{\partial t} + \frac{\partial n}{\partial l} \frac{\partial l}{\partial t} \right) = \frac{A}{2\sqrt{n}} \left(\frac{\partial n}{\partial t} + \frac{\partial n}{\partial l} v \right), \quad (2)$$

where coefficient $A = \frac{\alpha}{2\pi} \sqrt{\frac{4\pi e^2}{m}}$, $\alpha = 2$ for the harmonic, $\frac{\partial n}{\partial t}$ describes how the plasma density changes with time, $\frac{\partial n}{\partial l}$ is an electron density gradient along the path through which the exciter moves with velocity v . The equation can be rewritten as $df/dt \approx 2\Delta f \left(\frac{1}{\tau_{ssp}} - \frac{v}{\Delta l} \right)$, where (τ_{ssp}) is a temporal scale of density change.

Generally, only the second term $\frac{\partial n}{\partial l} v$, is considered in the interpretations of drifting bursts. For the frequency drift 3.6 GHz s^{-1} and $\Delta l = 1.5 \text{ Mm}$ the

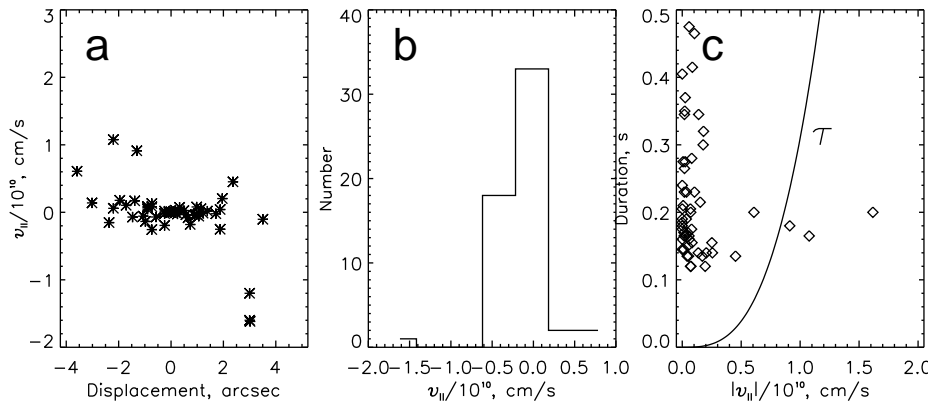


Figure 6. (a) Exciter velocities v vs. displacements Δl ; northward motion is positive. (b) Histogram of exciter velocities. (c) Relationship between the calculated absolute values of the exciter velocities and the total durations of drifting bursts. The solid curve shows calculated lifetimes τ .

exciter velocity is rather small (3×10^7 cm s $^{-1}$) compared to a velocity of nonthermal emitting electrons. The dependences in Figure 6 are calculated in the approximation of $2\Delta f/\tau_{\text{ssp}} = 3.6$ GHz/s. For density growth rate $\partial n/\partial t \approx 0.6 \times 10^{11}$ cm $^{-3}$ s $^{-1}$ the velocity along the loop tends to zero. Therefore, this value is the upper limit of the density growth rate.

The exciter velocity is found to be in the range -1.6 to 1.2×10^{10} cm s $^{-1}$, but for most pulses the longitudinal component of the velocity is less than 3×10^9 cm s $^{-1}$. The upper estimate of the life-time is determined by the Coulomb collisions ($\tau = 3.1 \times 10^{-20} v^3/n$; Trubnikov, 1965; Benz, 1993) and is shown by a solid line in Figure 6c. The diamonds denote observable pulse durations. The observable durations considerably exceed the electron life-times estimated from energies calculated as $mv_{||}^2/2$. In this case we must assume for most pulses that the transverse velocity of the emitting electrons is larger than the longitudinal velocity component. So the electrons are mainly accelerated across the magnetic field. Note that influence of relativistic effects on the velocity measurements caused by a velocity component along the line of sight is rather small because of the low exciter velocity and the small cross-section size of the emission region.

The analysis showed that the derived distributions in Figure 6b,c with and without taking into account the first term of Equation (2) are very similar to ones found for 30 March 2001. In other words the most of the electrons are definitely accelerated across magnetic field.

Usually the observation of type III-like bursts is considered as direct evidence of electron beams propagating in the solar corona. At large pitch-angle anisotropy of the emitting electrons and small exciter velocities along the loop the most likely mechanism should be loss-cone instabilities. Such distribution is able to excite hybrid plasma waves (Stepanov *et al.*, 1974; Zaitsev *et al.*, 1983; Fleishman and Melnikov, 1998). Electromagnetic emission at the double plasma frequency should be produced due to the nonlinear interaction between upper

hybrid waves. In this paper we did not discuss the emission mechanism in detail because there are a number of publications on this subject.

The modern models based on magnetic reconnection processes assume electron acceleration in multiple acceleration sites (Zharkova *et al.*, 2011; Lin, 2011). Rapid variations in flare emissions imply that reconnection is non-steady and a time-varying electric field is present in a reconnecting current sheet (Litvinenko, 2003). Multiple episodes of accelerations can be produced by repetitive interactions of multiple magnetic islands formed in regions either at the top of single helmet-like loop or at the intersection of interacting loops (Drake, 2006; Bárta, 2011).

It is reasonable to suggest that an individual drifting burst is a response to elementary energy release. In compressible plasma the pulses of electron acceleration should be accompanied by density growths at the reconnection site (Priest and Forbes, 2000). This explains the observed positive frequency drift pulses if the acceleration and reconnection sites are coincide.

6. Conclusions

The flare of 14 Apr 2002 with tens of short drifting bursts simultaneously recorded by the SSRT and wide-band spectropolarimeters SBRs was analyzed. The SSRT have recorded the sources of the drifting bursts simultaneously at two frequencies (5.67 and 5.76 GHz) which allowed us to distinguish between the spatial and temporal characteristics. The measured drift rates are clustered around value of 3.6 GHz s^{-1} . It was shown that the sources with emitting electrons are located inside a compact dense region near the loop top. The sizes of the acceleration region does not exceed a few Mm. Thus, observations and analyses of short-duration microwave drifting bursts provide a meaningful method to obtain information on the magnetic reconnection process. We hope that future spectrometers operating in a wide frequency range will provide us with a greater number of events for research.

Acknowledgement

We are grateful to the teams of Nobeyama Radio Observatory, RSTN, who have provided free access to their data. The authors thank the anonymous referee for useful suggestions. The research carried out by Robert Sych at NAOC was supported by the Chinese Academy of Sciences Visiting Professorship for Senior International Scientists, grant No. 2010T2J24. The research by Yihua Yan and Chengming Tan was supported by NSFC and MOST grants (10921303, 2011CB811401). This study was supported by the Russian Foundation of Basic Research (12-02-91161, 12-02-00173, 12-02-10006) and by a Marie Curie International Research Staff Exchange Scheme Fellowship within the 7th European Community Framework Programme. The work is supported in part by the grants of Ministry of education and science of the Russian Federation (State Contracts 16.518.11.7065 and 02.740.11.0576).

References

- Altyntsev, A.T., Grechnev, V.V., Konovalov, S.K.: 1996, *Astrophys. J.* **469**, 976.
- Altyntsev, A.T., Nakajima, H., Takano, T., Rudenko, G.V.: 2000, *Solar Phys.* **195**, 401.
- Altyntsev, A.T., Kuznetsov, A.A., Meshalkina, N.S., Yan, Y.: 2003a, *Astron. Astrophys.* **411**, 263.
- Altyntsev, A.T., Lesovoi, S.V., Meshalkina, N.S., Sych, R.A., Yan, Y.: 2003b, *Astron. Astrophys.* **400**, 337.
- Altyntsev, A.T., Grechnev, V.V., Meshalkina, N.S., Yan, Y.: 2007, *Solar Phys.* **242**, 111.
- Aschwanden, M.J. and Gudel, M.: 1992, *Astrophys. J.* **401**, 736.
- Aschwanden, M.J.: 1993, *Astrophys. J.* **417**, 790.
- Aschwanden, M.J., Dennis, B.R., Benz, A.O.: 1998, *Astrophys. J.* **497**, 972.
- Aschwanden, M.J.: 2002, *Space Sci. Rev.*, **101**, 1.
- Aschwanden, M.J.: 2004, *Astrophys. J.* **608**, 554.
- Bárta, M.; Büchner, J.; Karlický, M.: 2011, *Astrophys. J.* **737**, 24.
- Benz, A.O., Magun, A., Stehling, W., Su, H.: 1992, *Solar Phys.* **141**, 335.
- Benz, A.O.: 1993, *Plasma Astrophysics*, Kinetic Processes in Solar and Stellar Coronae, Dordrecht: Kluwer Academic Publishers.
- Benz, A.O.: 2000, in *Encyclopedia of Astronomy and Astrophysics*, (ed. Paul Murdin), Institute of Physics Publishing, Grove's Dictionaries, Inc., New York, **3**, 2553.
- Benz, A.O.: 2006, in: H. Rucker, W. Kurth, G. Mann (eds.) *Planetary and solar radio emissions VI*, 325.
- Delaboudiniere, J.-P., Artzner, G.E., Brunaud, J., Gabriel, A.H., Hochedez, J.F., Millier, F.F., et al.: 1995, *Solar Phys.*, **162**, 291.
- Drake, J.F., Swisdak, M., Che, H., Shay, M.A.: 2006, *Nature*, **443**, 553.
- Dulk, G.A.: 1985, *Astron. Astrophys.*, **23**, 169.
- Fleishman, G.D., Melnikov, V.F.: 1998, *Physics Uspekhi*, **41(12)**, 1157.
- Fleishman, G.D., Kuznetsov, A.A.: 2010, *Astrophys. J.*, **721**, 1127.
- Fleishman, G.D., Kontar, E.P., Nita, G.M., Gary, D.E.: 2011, *Astrophys. J. Lett.*, **731**, L19.
- Fu, Q., Qin, Z., Ji, H., Pei, L.: 1995, *Solar Phys.*, **160**, 97.
- Grechnev, V.V., Lesovoi, S.V., Smolkov, G.Ya., Krissinel, B.B., Zandanov, V.G., Altyntsev, A.T. et al.: 2003, *Solar Phys.*, **216**, 239.
- Huang, G.L., Fu, Q.J., Qin, Z.H.: 1999, *Astrophys. Space Sci.* **266**, 389.
- Ji, H., Fu, Q., Liu, Y., Cheng, C., Chen, Z., Yan Y., Zheng L., Ning Z., Tan, C., Lao, D.: 2003, *Solar Phys.*, **213**, 359.
- Kliem, B.: 1989, in Proc. International School and Workshop on Reconnection in Space Plasma, Vol.2, **ESA SP-285**, 117.
- Kliem, B.: 1995, in Proc. CESRA Workshop Held in Caputh/Potsdam, Germany (Berlin: Springer), 1995, p. 93.
- Kliem, B., Karlicky, M., Benz, A.O.: 2000, *Astron. Astrophys.*, **360**, 715.
- Lin, R.P.: 2011, *Space Sci. Rev.* **159**, 421.
- Litvinenko, Y.E.: 2003, *Solar Phys.*, **216**, 189.
- Machado, M.E., Ong, K.K., Emslie, A.G., Fishman, G. J., Meegan, C., Wilson, R., Paciasas, W.S.: et al.: 1993, *Adv. Space Res.*, **13**, 175.
- Meshalkina, N.S., Altyntsev, A.T., Sych, R.A., Chernov, G.P., Yihua Y.: 2004, *Solar Phys.*, **221**, 85.
- Meshalkina, N.S., Altyntsev, A.T., Lesovoi S.V., Zandanov, V.G.: 2004, *Adv. Space Res.*, **35(10)**, 1785.
- Nakajima, H., Sekiguchi, H., Sawa, M., Kai, K., Kawashima, S.: 1985, *Publ. Astron. Soc. Japan*, **37**, 163.
- Nakajima, H., Nishio, M., Enome, S., Shibasaki, K., Takano, T., Hanaoka, Y., Torii, C., Sekiguchi, H., Bushimata, T., Kawashima, S., Shinohara, N., Irimajiri, Y., Koshiishi, H., Kosugi, T., Shiomi, Y., Sawa, M., and Kai, K.: 1994, in Proc. IEEE **82(5)**, 705.
- Priest, E. and Forbes, T.: 2000, *Magnetic reconnection*, Cambridge: Cambridge Univ. Press, 612.
- Robinson, P.A. and Benz, A.O.: 2000, *Solar Phys.*, **194**, 345.
- Scherrer, P.H., Bogart, R.S., Bush, R.I., Hoeksema, J.T., Kosovichev, A.G., Schou, J., et al.: 1995, *Solar Phys.*, **162**, 129.
- Shibasaki, K., Ishiguro, M., Enome, S.: 1979, *Nagoya University, Research Institute of Atmospheric Sciences, Proceedings*, **26**, 117.

- Stepanov, A. V.: 1974, *Soviet Astron.*, **17**, 781.
Torii, C., Tsukiji, Y., Kobayashi, S., Yoshimi, N., Tanaka, H., Enome, S.: 1979, *Proc. Res. Inst. Atmospheric, Nagoya Univ.*, **26**, 129.
Trubnikov, B.A.: 1965, *Rev. Plasma Phys.*, **1**, 105.
Zaitsev, V.V., Stepanov, A.V.: 1983, *Solar Phys.*, **88**, 297.
Zharkova, V.V.; Arzner, K.; Benz, A.O. *et al.*: 2011, *Space Sci. Rev.*, **159**, 357.

